# Nanoscale

Accepted Manuscript


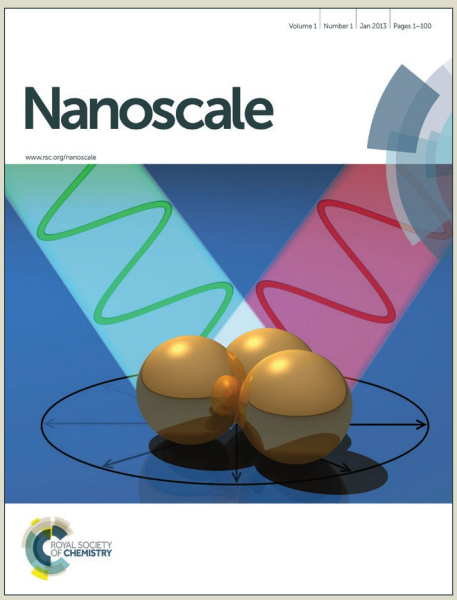





ROYAL SOCIETY OF CHEMISTRY

www.rsc.org/nanoscale

# On-Surface Synthesis of Two-dimensional Imine Polymers with Tunable Band Gap: a Combined STM, DFT and Monte Carlo Investigation

Lirong Xu,[†¶] Yanxia Yu,[†] Jianbin Lin,[⊥] Xin Zhou,[§*] Wei Quan Tian,[§] Damian Nieckarz,[‡] Pawel Szabelski,[‡*] Shengbin Lei,[†§*]

[†] State Key Laboratory of Robotics and System (HIT), Harbin Institute of Technology, Harbin, 150080, People's Republic of China, Email: leisb@hit.edu.cn, zhoux@hit.edu.cn

[‡] Department of Theoretical Chemistry, Maria-Curie Skzodowska University, Pl. M.C. Skzodowska, 3, 20-031 Lublin, Poland, Email: szabla@vega.umcs.lublin.pl

[⊥] Department of Chemistry, College of Chemistry and Chemical Engineering, and MOE Key Laboratory of Analytical Sciences, Xiamen University, Xiamen 361005, China

[§]Department of Chemistry, School of Science & Collaborative Innovation Center of Chemical Science and Engineering (Tianjin), Tianjin University, Tianjin 300072, People's Republic of China

[¶]School of Chemistry and Chemical Engineering, Qufu Normal University, Qufu 273165, Shandong, China.

**ABSTRACT**

Two-dimensional polymers are of great interest for many potential applications in nanotechnology. Preparation of crystalline 2D polymers with tunable band gap is critical for its applications in nano-electronics and optoelectronics. In this work, we try to tune the band gap of 2D imine polymers by expanding the conjugation of the backbone of aromatic diamines both laterally and longitudinally. STM characterization reveals that the regularity of the 2D polymers can be affected by the existence of lateral bulky groups. Density functional theory (DFT) simulations discovered a significant narrowing of the band gap of imine 2D polymers upon the expanding of conjugation of monomer backbone, which has been confirmed experimentally by UV absorption measurements. Monte Carlo simulations help us to put further insight into the controlling factors on the formation of regular 2D polymers, which demonstrated that based on the all rigid assumption, the coexistence of different conformations of the imine moiety has significant effect on the regularity of the imine 2D polymers.

**KEYWORDS:** On-surface reaction; 2D polymer; imine; tunable band gap; STM

## INTRODUCTION

Recently, the realization of long-range ordered single layer two-dimensional (2D) polymers has attracted significant interest due to its potential applications in the field of electronic, photoelectronic materials *etc*.[1-3] Up to now, different types of 2D polymers have been accomplished through on-surface synthesis on single crystalline substrates, such as condensation and esterification of boronic acids,[4,5] Ulmann coupling,[6-8] Schiff-base coupling, *etc*.[9,10] Single layer of π-conjugated 2D polymers represent one class of intriguing 2D materials due to the efficient in-plane electron transport through covalent bond,[11] which can be applied in the field of nanoelectronics and photoelectronics as an alternation of graphene[12-15] and transition-metal dichalcogenide.[16]

π-Conjugated 2D polymers are 2D organic semiconductors.[17] The electronic structure of the 2D polymer can be tuned by alternating their backbone structure or introducing functional groups onto the backbone.[18-21] π-Conjugated polymers can be used as the active material in optoelectronic devices. The optical, electrical and other characteristics of conjugated polymers are determined by its electronic structure. The research on the characteristics of chemical and electronic structure of conjugated polymers is meaningful for exploring their applications in the field of field-effect transistors, solar cells *etc*.[22-24] Theoretical calculations have predicted that the electronic structures of conjugated 2D polymers can be adjusted by tuning the topology and the periodicity of materials.[25,26] The "band gap tuning" may give conjugated 2D polymers with desired optical and electrical properties.[27]

In our previous work, we have demonstrated a simple preparation protocol for the synthesis of regular 2D polymers through on-surface Schiff-base coupling of benzene-1,3,5-tricarbaldehyde (BTA) with four different linear aromatic diamines on

an inert highly oriented pyrolytic graphite (HOPG) surface,[28] we now extend the same strategy to grow 2D imine polymers with tunable band gap by extending the conjugation of monomer backbone. On basis of the previous investigation, in our present work, we try to extend the conjugation in two dimensions: the width or the length of the diamine. The molecular structures of four diamine monomers are illustrated in Scheme 1. On the basis of PDA, we replace it with (4-amino-1-naphthyl) amine (DAN), in which the benzene ring was replaced with naphthalene to extend the conjugation; benzidine, in which the length of the backbone is extended; and AABA, in which the backbone is extended both laterally and longitudinally. All of the precursors can form longe-range 2D polymers on HOPG surface via on-surface Schiff-base coupling with BTA. The conformation and electronic structure of the 2D polymers were first investigated with density functional theory (DFT), and the on-surface synthesis was performed on HOPG surface and the structure was characterized by scanning tunneling microscopy (STM). And then, the optical band gap of these 2DPs were experimentally determined by UV-Vis spectroscopy. In addition, Monte Carlo simulations were also performed to put an insight into the underlying mechanism controlling the ordering of these 2D polymers.

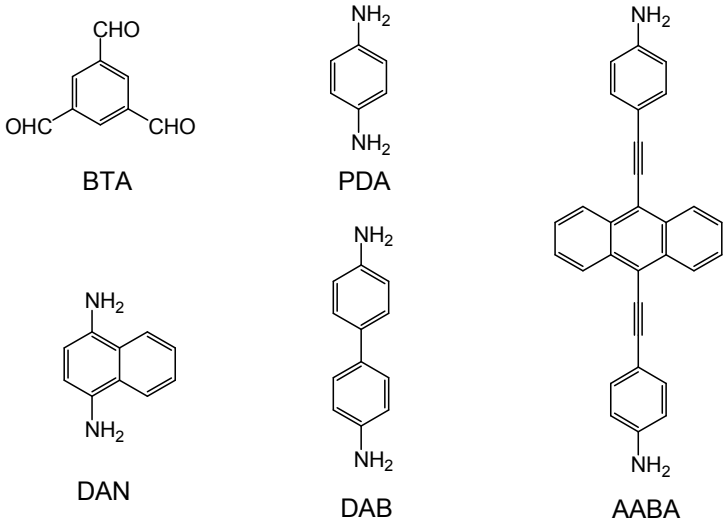

**Scheme 1.** Molecular structure of monomers. Benzene-1, 3, 5-tricarbaldehyde (BTA); *p*-Phenylenediamine (PDA); (4-amino-1-naphthyl) amine (DAN); Benzidine (DAB); 4-(2-(9-(2-(4-aminophenyl)ethynyl)anthracen-10-yl)ethynyl) benzenamine (AABA).

## RESULTS AND DISCUSSION

### Density Functional Theory Simulations

To verify how the planarity of the surface COFs and the lateral dimension of monomer conjugation influence the band gap of 2D polymers, we have first carried out DFT simulations on the geometrical and electronic structure of the expected 2D polymers. Figure 1 shows geometrical structures of the target 2D polymers. The unit cell of the 2D polymers is hexagonal with dimensions of a = b = 22.5 Å ($2DP_{BTA\text{-}PDA}$), a = b = 22.4 Å ($2DP_{BTA\text{-}DAN}$), a = b = 30.1 Å ($2DP_{BTA\text{-}DAB}$), a = b = 46.5 Å ($2DP_{BTA\text{-}AABA}$). All of the bond lengths fall in the normal range of C–C, C–N and C–H bonds.[28,29] The side view of the optimized conformations indicates that the $2DP_{BTA\text{-}DAN}$ has the best planarity, in which all atoms are on the same plane, while the other three 2D polymers are more or less nonplanar, especially $2DP_{BTA\text{-}DAB}$. The dihedral angles are indicated in Figure 1. As a result of the repulsion between hydrogens on the neighboring phenyl ring, a large dihedral angle exists between the two phenyl rings, hence one phenyl group being out of the molecular plane. Figure 2 shows the band structures of the 2D polymers. The DFT simulation gives a band gap of 2.041 eV for $2DP_{BTA\text{-}PDA}$, while replacing PDA with DAB only leads to a neglectable decrease to 2.002 eV. This is possibly due to the rotation of the phenyl group which affected the extension of the conjugation. Instead, the band gap of $2DP_{BTA\text{-}DAN}$ significantly decreased to 1.658 eV due to the lateral extension of the

backbone and the good planarity of the 2D polymer. The π-conjugation and the planar structure all contribute to the decrease of $2DP_{BTA\text{-}DAN}$ band gap. The extension of conjugated backbone of AABA causes a further narrowing of the band gap of $2DP_{BTA\text{-}AABA}$ to 1.263 eV. The DFT calculation suggests that the lateral expanding of conjugation can significantly decrease the band gap of the 2D polymers, which is consistent with the previous theoretical simulations,[18,19] and has been confirmed experimentally by our following UV-Vis absorption measurements.

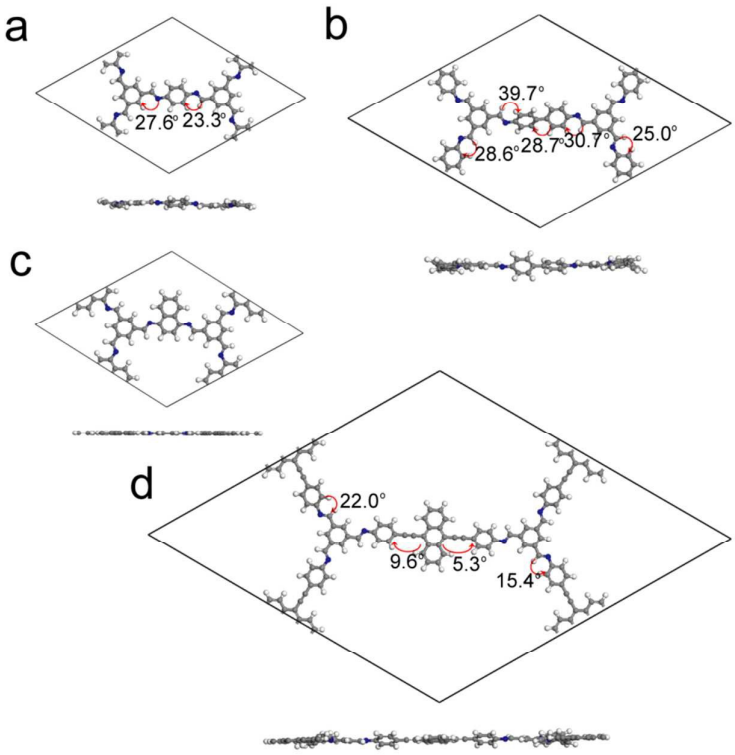


**Figure 1.** Geometrical structures of (a) $2DP_{BTA\text{-}PDA}$, (b) $2DP_{BTA\text{-}DAB}$, (c) $2DP_{BTA\text{-}DAN}$, and (d) $2DP_{BTA\text{-}AABA}$ in unit cell (top and side views).

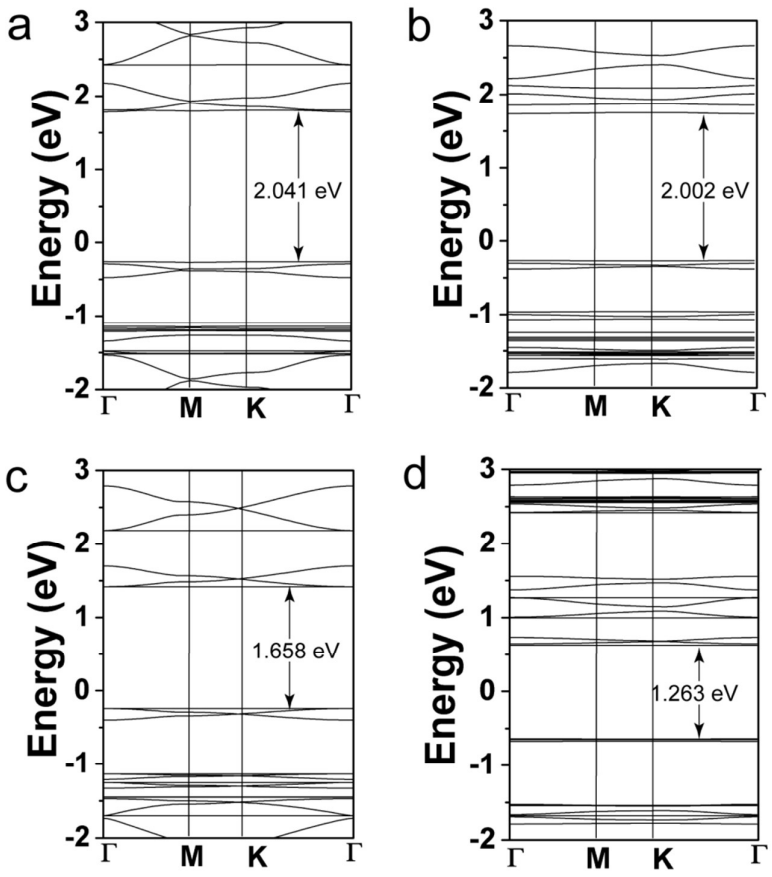


**Figure 2.** The band structure of (a) $2DP_{BTA\text{-}PDA}$, (b) $2DP_{BTA\text{-}DAB}$, (c) $2DP_{BTA\text{-}DAN}$, and (d) $2DP_{BTA\text{-}AABA}$.

**On-surface Synthesis and Band Gap Evaluation**

The Schiff-base coupling at the gas/solid interface was carried out in a vacuum oven at 140 °C with a base pressure of <133 Pa, following the same protocol as reported in one of our previous work.[28] For the on-surface synthesis of $2DP_{BTA\text{-}DAN}$ on HOPG substrate, according to the method that we have reported, BTA and DAN were dissolved in DMSO with a mole ratio of about 1:3 and drop-casted onto the substrate surface.[29] In order to promote the reversibility of the on-surface Schiff base reaction,[31,32] a small amount of deionized water was added in the solution. Annealing the sample at 140 °C for 30 min results in a network with reasonable long-range order,

which can be reflected from the two-dimensional fast Fourier transformation (FFT) of the STM image (Figure 3a and inset).

However, high resolution STM image still reveals unperfection of the network, (Figure 3b). High density topological defects can be distinguished in the STM image, and the crystalline domain of $2DP_{BTA\text{-}DAN}$ is small in comparison with that of $2DP_{BTA\text{-}PDA}$ and $2DP_{BTA\text{-}DAB}$ (Figure S1). Despite the presence of defects, the topography of $2DP_{BTA\text{-}DAN}$ is dominated by hexagonal network. The network has a periodicity of 2.2 ± 0.1 nm, identical to that of $2DP_{BTA\text{-}PDA}$ within experimental error. However, due to the existence of naphthalene group the diameter of the hexagonal pore decreases to ~1.5 nm.

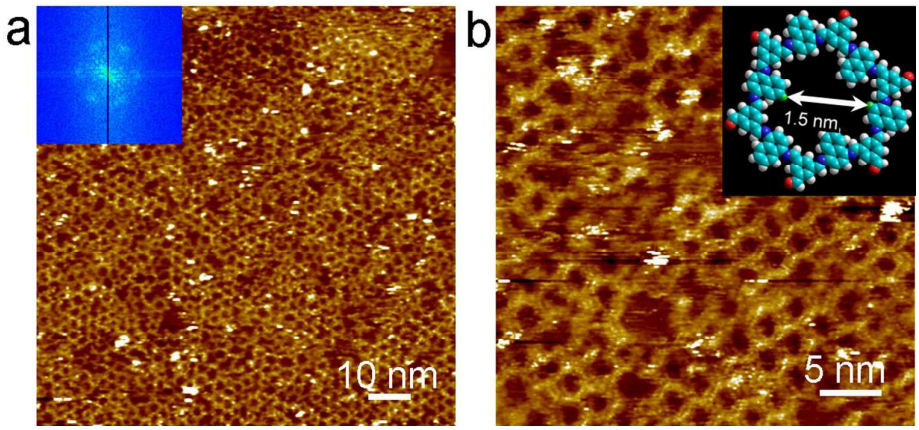


**Figure 3.** (a) Large-scale STM image of $2DP_{BTA\text{-}DAN}$ obtained in presence of deionized water, with the inset depicting the corresponding FFT spectrum of the STM image. (b) High resolution STM image of $2DP_{BTA\text{-}DAN}$ with the inset depicting the chemical structure of a hexagonal pore, the diameter of the hexagonal pore was indicated by a white arrow. The tunneling conditions were I = 0.500 nA, V = 0.500 V.

The Schiff-base coupling of BTA and AABA was carried out by mixing both of the monomers in DMSO and then put the sample in a vacuum oven at 140 °C for 4 h with

a base pressure of <133 Pa. A single layer of $2DP_{BTA\text{-}AABA}$ can be obtained with nearly full surface coverage on HOPG surface (Figure 4). Though only small regular domains can be observed, the FFT of the image still exhibits six scattered spots, suggests some kind of long-range order. The high resolution STM image of $2DP_{BTA\text{-}AABA}$ indicates the anthracene group in the AABA moiety exhibit higher contrast in comparison with the other parts. The periodicity of $2DP_{BTA\text{-}AABA}$ extends to 4.6 ± 0.1 nm, due to the extended length of the *p*-phenyleneethynylene backbone. The observed periodicity of the $2DP_{BTA\text{-}AABA}$ agrees well with that expected from the DFT calculation, confirming the covalent bond formation. The diameter of the hexagonal pore of $2DP_{BTA\text{-}AABA}$ is 3.6 ± 0.1 nm.

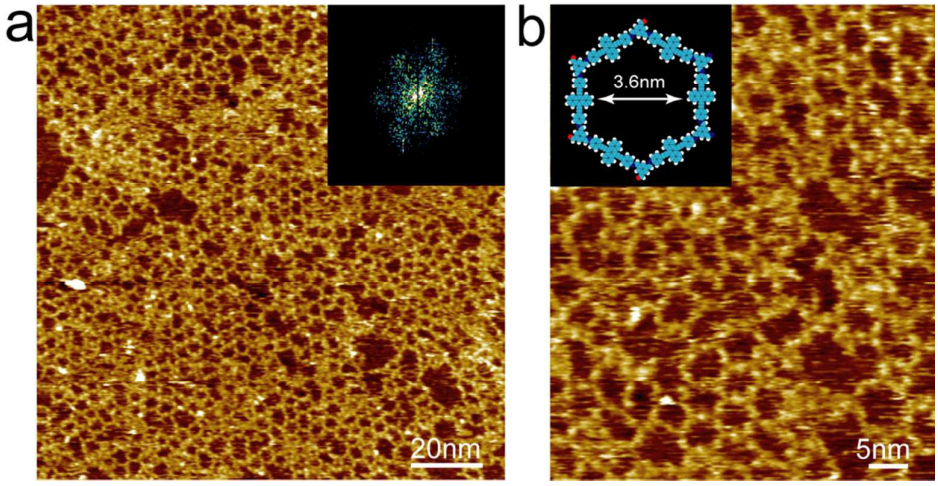


**Figure 4.** (a) Large-scale and (b) High resolution STM image of $2DP_{BTA\text{-}AABA}$. The inset in (a) and (b) shows the FFT of the STM image and depicting the chemical structure of an ideal hexagonal pore of $2DP_{BTA\text{-}AABA}$, respectively. The diameter of the hexagonal pore was indicated by a white arrow. The tunneling conditions were I = 0.025 nA, V = -0.600 V.

What worth mentioning is that though the construction of covalent networks with large periodicity is essential for the application of 2D polymers as nanopatterning,

nanoreactors and nanotemplates, its large porosity leads to inherent instability and makes the construction of such networks difficult. We find out that the success of $2DP_{BTA\text{-}AABA}$ relies sensitively on the concentration of monomers. Porous networks as shown in Figure 5 can only be obtained with rather low monomer concentration. Increasing the monomer concentration will lead to networks filled with AABA monomers and incompletely polymerized linear/zigzag polymers and oligomers (Figure S2). In fact even in the network obtained with quite low monomer concentration as in Figure 5, pore filling with unreacted monomers can still be occasionally observed.

In comparison with the polyphenyl backbone of PDA and DAB, the *p*-phenyleneethynylene backbone of AABA has very good planarity which favors the extension of two-dimensional conjugation in $2DP_{BTA\text{-}AABA}$, but in the same time, it increases the π-π stacking with HOPG substrate and significantly increases the adsorption energy and in turn affects the mobility of AABA on the surface. This also applies to the DAN monomer, and this decrease in monomer mobility on the surface will hinder the formation of extended regular 2D polymers and might be one reason for the decreased regularity of $2DP_{BTA\text{-}DAN}$ and $2DP_{BTA\text{-}AABA}$.

The band gap of organic semiconductors can be experimentally evaluated by optical or electrochemical methods, for instance, UV-Vis spectroscopy and cyclic voltammetry (CV).[33-34] In this work the band gap of the synthesized 2DPs were experimentally evaluated by UV-Vis spectroscopy. The so called optical band gap can be estimated either by the onset wavelength or maximum absorption wavelength, and comparing with the ill-defined onset value, the maximum absorption wavelength is more widely used. According to the UV-Vis spectrum of the 2DPs (Figure S3), the band gap values were determined to be, 3.10 eV for $2DP_{BTA\text{-}PDA}$, 3.16 eV for

$2DP_{BTA\text{-}DAB}$, 2.90 eV for $2DP_{BTA\text{-}DAN}$, 2.58 eV for $2DP_{BTA\text{-}AABA}$. Though the optical band gaps determined from the absorption spectrum are larger than the values from the DFT simulation, the trend is in good agreement with the theoretical prediction and confirms that our design strategy is viable. The difference between the experimentally determined and DFT simulated band gap may partly due to the difference in sample preparation conditions (higher concentration, different substrate, which lack of epitaxy effect, etc.). The higher monomer concentration used for the preparing of UV-Vis sample and lack of epitaxy effect on quartz glass may significantly reduce the degree of polymerization, leads to larger band gap. Another issue needs to pay attention is the effect of defects. As revealed by the STM characterizations, a lot of defects exist in the 2D imine polymers. Some experience from other 2D materials suggest some defect related states may emerge between the frontier bands, and thus actually decrease the band gap of the material. A recent theoretical work on the electronic structure and transport properties of 2D polymers indicates significant influence of defects on the electronic structure and transport properties of the organic 2D polymers.[35] However, the actual effect of such defects on the properties of 2D imine polymers still awaiting for further investigations, both from theoretical and experimental aspects.

**Monte Carlo Simulation**

To further understand the mechanism of the on-surface polymerization process, computer simulations were carried out on the BTA-DAN system using the lattice gas cannonical Monte Carlo (GCMC) method which was described in detail in the Supporting Information section.[36-38] The simplified models of the three conformations, *cis-egzo*, *cis-endo* and *trans*, of imine moiety are shown in Figure 5a, where the trans

conformation has two enantiomers when adsorb on the surface, denoted as *trans R* and *trans L*, respectively. According to our DFT simulations, these conformations exhibit different stability on the surface due to repulsion between the $H_{imine}$ and H5/H8 (Figure S4), thus we have assumed different stability of these conformations in the Monte Carlo simulation, and Figure 5b shows a snapshot of the 2D polymer when the stability of these conformations is set as $E_{cis\text{-}egzo} = -2.00$, $E_{trans} = -1.95$ and $E_{cis\text{-}endo} = -1.90$ (in kT units). In this network these three conformations coexist, which results in a decrease in regularity. Figure 5c shows statistics of the occurrence of these conformations in the network. The most stable *cis-egzo* conformation only show a slight preference than the *trans* conformation, and the most unstable *cis-endo* conformation also has an about 18% probability to appear in the network. Further increase of the difference in relative stability to $E_{cis\text{-}egzo} = -2.00$, $E_{trans} = -1.90$ and $E_{cis\text{-}endo} = -1.80$ (in kT units) increases the preference toward the *cis-egzo* conformation (Figure S5b) but has moderate effect on the regularity of the networks. In this case, appearance of the other conformations is not precluded. These results indicate the coexistence of different conformations of the imine moiety might be one reason for the low regularity of the 2D imine polymers.

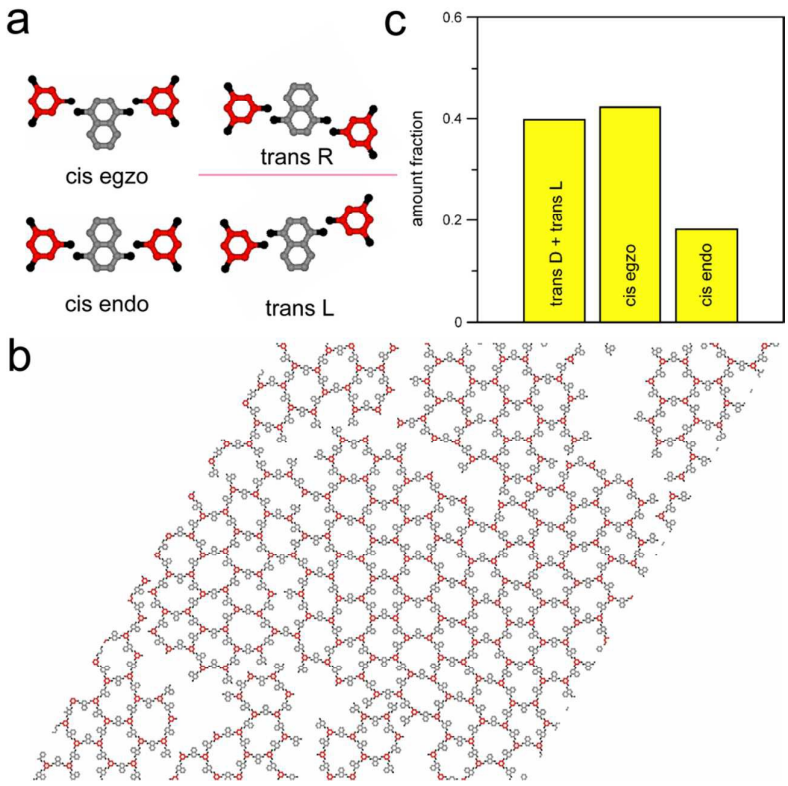


**Figure 5.** (a) Simplified model of different conformations of the imine moiety of $2DP_{BTA\text{-}DAN}$, (b) Monte Carlo snapshot of the $2DP_{BTA\text{-}DAN}$ formed with settings of $E_{cis\text{-}egzo} = -2.00$, $E_{trans} = -1.95$ and $E_{cis\text{-}endo} = -1.90$ (in $kT$ units), (c) relative abundance of different conformations in the 2D polymer.

We have also adapted extreme settings to see what kind of network will form if some of the conformations are precluded. Figure 6a shows a snapshot where only the *cis-egzo* conformation is allowed. In this case the alignment of BTA units (red hexagons) is perfectly regular, forming an ideal honeycomb network. However, the orientation of the naphthalene group is still random, making the network aperiodic. Three extreme cases are enlarged as shown in the upper left to lower right corners of Figure 6a with all naphthalene groups pointing inside, arranged alternately and all pointing outside the hexagon, respectively. Only with the six naphthalene unit point alternately inside and outside the hexagon ring the network can be ideally periodic.

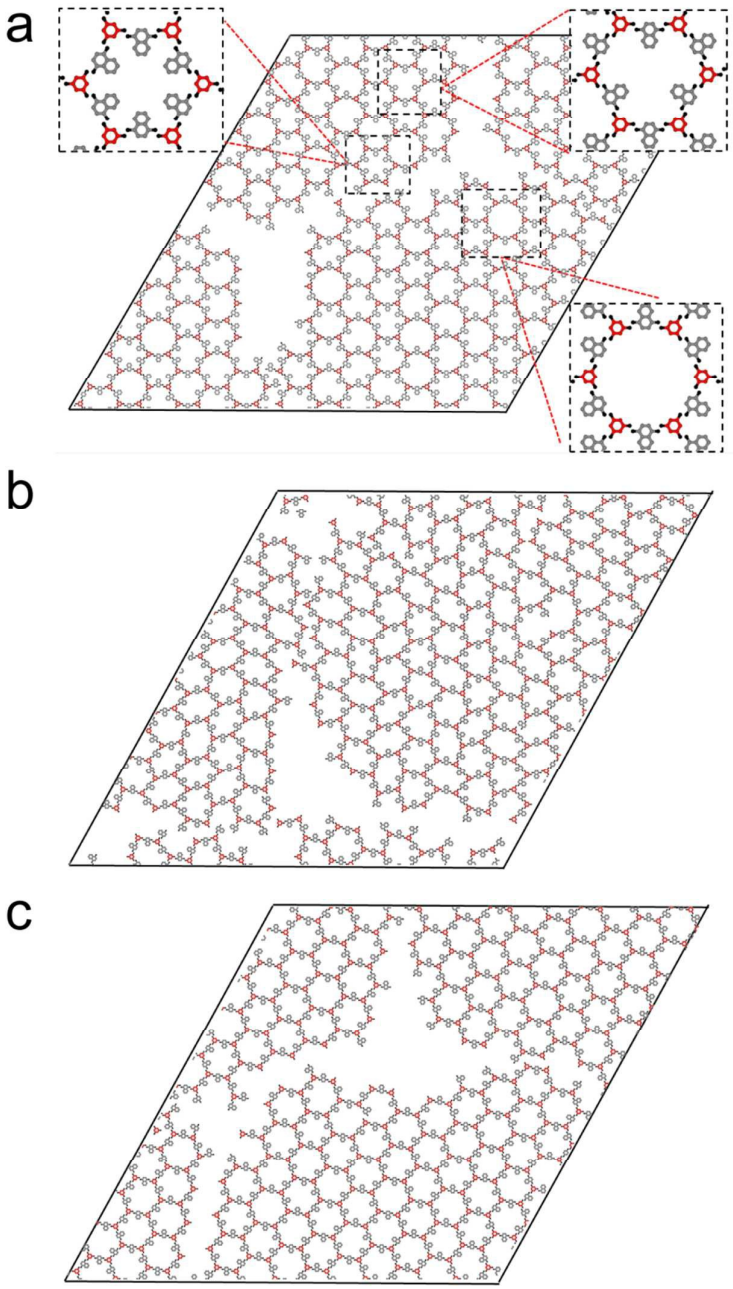


**Figure 6.** Monte Carlo snapshots of the $2DP_{BTA\text{-}DAN}$ formed with settings of (a) $E_{cis\text{-}egzo}$ = –2.00 kT units, (b) $E_{trans}$ = –2.00 kT units, (c) $E_{trans\ R}$ = –2.00 kT units.

As shown in Figure 6b, when both *cis* conformations are precluded but the two enantiomers of *trans* conformation are present in the network, the random mixing of both enantiomers leads to irregularity to the network. Only in the case as shown in

Figure 6c, when just *trans R* enantiomer is allowed, the network is ideally regular if we ignore the orientation of the naphthalene groups. In summary, according to these simulations only when just one conformation is allowed the surface confined Schiff base reaction can lead to highly regular 2D polymer. Certainly, when DAN is replace by PDA, then there is only one possible *cis* conformation and the issue of naphthalene orientation does not exist, then the network as shown in Figure 6a and 6c will be ideally periodic. One thing worth mentioning is that our Monte Carlo simulation is based on the assumption that the units are strictly rigid and the interactions between them are strictly directional. However, in reality the stiff resistance of the conjugated backbone is limited and bond angles can be altered in a small range with neglectable energy penalty, thus coexistence of different conformations, at least with small portion, will not necessarily leads to distortion of the network.

## DISCUSSION AND CONCLUSIONS

In this work we report on a straight forward strategy for the on-surface synthesis of surface confined 2D polymers based on Schiff-base condensation with extended conjugated backbones, which may allow for tuning their band gaps. The STM characterizations reveal that the regularity of the 2D polymers can be affected by the existence of lateral bulky groups and the decreased mobility due to the stronger interaction with the substrate.

DFT simulations revealed a significant narrowing of the band gap of $2DP_{BTA\text{-}DAN}$ and $2DP_{BTA\text{-}AABA}$ due to extended conjugation, which have been confirmed experimentally by UV-Vis measurements, thus confirms that our design strategy is viable. The DFT calculation suggests that both the planarity of the 2D polymer and the lateral dimension of monomer conjugation has important influence on the band gap. On the other hand, Monte Carlo simulations give insight on a large scale how the

coexistence of different conformations of the imine moiety can influence the regularity of the 2D imine polymer. It suggests, based on the assumption that the building unit are totally rigid and the connections are strictly directional, only when just one conformer is allowed the 2D polymer can be ideally regular.

The results provide valuable information for the design and synthesis of regular surface confined 2D polymers with desired chemical and electronic structures which is important for the application of this type of facilitating 2D materials in the field of optoelectronic devices.

## MATERIAL AND METHEDS

BTA, DAN, dimethylsulfoxide (DMSO) were purchased from J&K and used without further purification. AABA was synthesized according to reported method.[37] For sample preparation of $2DP_{BTA\text{-}DAN}$ on HOPG surface, the monomers were first dissolved in DMSO with a mass concentration of 1 mg/g respectively. Then the aromatic amine and aldehyde were mixed with mole ratio of about 3:1. Then the solutions were diluted 100 times, a small amount of deionized water was added in the mixing solution of BTA and DAN with volume ratio 3:100. An amount of ~5 μL of the solution was drop-casted on the freshly cleaved surface of HOPG. The drop-cast samples were positioned in a preheated vacuum oven and annealing at 140 °C for 30 min. For sample preparation of $2DP_{BTA\text{-}AABA}$ on HOPG surface, the monomers were first dissolved in DMSO with a mass concentration of 1 mg/g respectively. Mix them with mole ratio of about 3:1. Then the solutions were diluted 500 times, a small amount of deionized water was added in the mixing solution of BTA and AABA with volume ratio 5:100. An amount of ~6 μL of the solution was drop-casted on the freshly cleaved surface of HOPG. The drop-cast samples were positioned in a

preheated vacuum oven and annealing at 140 °C for 4 h. The sample was characterized with STM at the solid/air interface at room temperature. STM measurements were performed on an Agilent 5100 Scanning Probe Microscopy with mechanically formed Pt/Ir (80/20) tips under ambient conditions. All images were taken with the constant current mode. The calibration of STM images were carried out by using HOPG lattice with atomic resolution. The chemical structure models were built by the HyperChem software.

UV absorption spectra were obtained using a UV-2700 UV-Vis spectrophotometer. The 2DP samples were prepared by drop-casting the mixed solution of corresponding monomers onto a quartz slice and annealed in the vacuum oven, similar as the samples for STM measurements. However, to get higher signal-to-noise ratio, the total concentration of monomers was increase to 0.1 mg/g.

State-of-the-art electronic structure calculations based on density functional theory with the project augmented wave method (PAW) were performed using the Vienna ab-initio simulation package (VASP).[40,41] Perdew-Burke-Ernzerh (PBE)[42] exchange-correlation potential was employed and a plane-wave basis set with a cut-off energy of 400 eV was used with a 3×3×1 point grid for the relaxation of structure and 8×8×1 k-point mesh for the electronic structure calculation. A vacuum region with thickness of 15 Å was used in the calculation to avoid the possible interaction between images.

To simulate the mixed self-assembly of amine (DAN) and dialdehyde (BTA) molecules we used the simplified lattice Monte Carlo model whose successful application to a wide class of 2D supramolecular systems was demonstrated in the previous works.[36-38] The details are discribed in the Supporting Information section.

***Acknowledgement.*** This work is supported by the National Science Foundation of

China (21373070, 21572157, 21303030), the Open Project of State Key Laboratory of Robotics and System (HIT) (SKLRS-2015-MS-11). WQT also thanks the Open Project of State Key laboratory of Supramolecular Structure and Materials (JLU) (SKLSSM201620).

***Supporting Information Available:*** Extra STM and Monte Carlo data. This material is available free of charge *via* the internet at http://pubs.acs.org.

**REFERENCES AND NOTES**

1. D. F. Perepichka, F. Rosei, *Science* **2009**, *323*, 216-217.
2. S. Blankenburg, M. Bieri, R. Fasel, K. Müllen, C. A. Pignedoli, D. Passerone, *Small* **2010**, *6*, 2266-2271.
3. A. Gourdon, *Angew. Chem. Int. Ed.* **2008**, *47*, 6950-6953.
4. N. A. A. Zwaneveld, R. Pawlak, M. Abel, D. Catalin, D. Gigmes, D. Bertin, L. Porte, *J. Am. Chem. Soc.* **2008**, *130*, 6678-6679.
5. J. F. Dienstmaier, D. D. Medina, M. Dogru, P. Knochel, T. Bein, W. M. Heckl, M. Lackinger, *ACS Nano* **2012**, *6*, 7234-7242.
6. L. Grill, M. Dyer, L. Lafferentz, M. Persson, M. V. Peters, S. Hecht, *Nat. Nanotech.* **2007**, *2*, 687-691.
7. J. C. Russell, M. O. Blunt, J. M. Garfitt, D. J. Scurr, M. Alexander, N. R. Champness, P. H. Beton, *J. Am. Chem. Soc.* **2011**, *133*, 4220-4223.
8. T. Dienel, J. Gómez-Díaz, A. P. Seitsonen, R. Widmer, M. Iannuzzi, K. Radican, H. Sachdev, K. Müllen, J. Hutter, O. Gröning, *ACS Nano* **2014**, *8*, 6571-6579.
9. R. Tanoue, R. Higuchi, N. Enoki, Y. Miyasato, S. Uemura, N. Kimizuka, A. Z. Stieg, J. K. Gimzewski, M. Kunitake, *ACS Nano* **2011**, *5*, 3923-3929.
10. X. H. Liu, C. Z. Guan, S. Y. Ding, W. Wang, H. J. Yan, D. Wang, L. J. Wan, *J. Am.*

*Chem. Soc.* **2013**, *135*, 10470-10474.

11. N. R. Champness, *Nat. Nanotech*. **2007**, *2*, 671-672.
12. L. Cardenas, R. Gutzler, J. Lipton-Duffin, C. Y. Fu, J. L. Brusso, L. E. Dinca, M. Vondráček, Y. Fagot-Revurat, D. Malterre, F. Rosei, D. F. Perepichka, *Chem. Sci.* **2013**, *4*, 3263-3268.
13. Y. G. Zhou, Z. G. Wang, P. Yang, X. T. Zu, F. Gao, *J. Mater. Chem.* **2012**, *22*, 16964-16970.
14. Y. T. Liang, M. C. Hersam, *Macromol. Chem. Phys.* **2012**, *213*, 1091-1100.
15. S. Z. Butler, S. M. Hollen, L. Y. Cao, Y. Cui, J. A. Gupta, H. R. Gutiérrez, T. F. Heinz, S. S. Hong, J. X. Huang, A. F. Ismach, E. Johnston-Halperin, M. Kuno, V. V. Plashnitsa, R. D. Robinson, R. S. Ruoff, S. Salahuddin, J. Shan, L. Shi, M. G. Spencer, M. Terrones, W. Windl, J. E. Goldberger, *ACS Nano* **2013**, *7*, 2898-2926.
16. D. Jariwala, V. K. Sangwan, L. J. Lauhon, T. J. Marks, M. C. Hersam, *ACS Nano* **2014**, *8*, 1102-1120.
17. H. A. M. van Mullekom, J. A. J. M. Vekemans, E. E. Havinga, E. W. Meijer, *Mater. Sci. Eng.* **2001**, *32*, 1-40.
18. R. Gutzler, D. F. Perepichka, *J. Am. Chem. Soc.* **2013**, *135*, 16585-16594.
19. P. Zhu, V. Meunier, *J. Chem. Phys.* **2012**, *137*, 244703.
20. N. C. Greenham, A. R. Brown, J. H. Burroughes, D. D. C. Bradley, R. H. Friend, P. L. Burn, A. Kraft, A. B. Holmes, *Chem. Phys. Lett.* **1992**, *200*, 46-54.
21. J. Cornil, D. Beljonne, D. A. dos Santos, Z. G. Shuai, J. L. Brédas, *Synthetic Metals* **1996**, *78*, 209-217.
22. K. Kudo, M. Lizuka, S. Kuniyoshi, K. Tanaka, *Thin Solid Films*, **2001**, *393*, 362-367.
23. C. Winder, G. Matt, J. C. Hummelen, R. A. J. Janssen, N. S. Sariciftci, C. J.

Brabec, *Thin Solid Films*, **2002**, *403-404*, 373-379.

24. L. Chen, L. S. Roman, D. M. Johansson, M. Svensson, M. R. Andersson, R. A. A. J. Janssen, O. Inganäs, *Adv. Mater.* **2000**, *12*, 1110-1114.
25. R. H. Baughman, H. Eckhardt, M. Kertesz, *J. Chem. Phys*. **1987**, *87*, 6687-6699.
26. F. F. Abraham, D. R. Nelson, *Science*, **1990**, *249*, 393-397.
27. J. Roncali, *Chem. Rev*. **1997**, *97*, 173-205.
28. L. R. Xu, X. Zhou, Y. X. Yu, W. Q. Tian, J. Ma, S. B. Lei, *ACS Nano* **2013**, *7*, 8066-8073.
29. L. R. Xu, X. Zhou, W. Q. Tian, T. Gao, Y. F. Zhang, S. B. Lei, Z. F. Liu, *Angew. Chem. Int. Ed.* **2014**, *53*, 9564-9568.
30. O. Ourdjini, R. Pawlak, M. Abel, S. Clair, L. Chen, N. Bergeon, M. Sassi, V. Oison, Jean-M. Debierre, R. Coratger, L. Porte, *Phys. Rev. B* **2011**, *84*, 125421.
31. J. F. Dienstmaier, A. M. Gigler, A. J. Goetz, P. Knochel, T. Bein, A. Lyapin, S. Reichlmaier, W. M. Heckl, M. Lackinger, *ACS Nano* **2011**, *5*, 9737-9745.
32. C. Z. Guan, D. Wang, L. J. Wan, *Chem. Commun*. **2012**, *48*, 2943-2945.
33. S. Admassie, O. Inganäs, W. Mammo, E. Perzon, M. R. Andsersson, *Synth. Met.*, 2006, 156, 614-623.
34. R. Holze, *Organometallics*, 2014, 33, 5033-5042.
35. J. J. Adjizian, A. Lherbier, S. M. M. Dubois, A. R. Botello-Méndez, J. C. Charlier, *Nanoscale*, **2016**, DOI: 10.1039/c5nr06825h.
36. P. Szabelski, S. De Feyter, M. Drach, S. B. Lei, *Langmuir* **2010**, *26*, 9506–9515.
37. S. Lei, K. Tahara, K. Müllen, P. Szabelski, Y. Tobe, S. De Feyter, *ACS Nano*, **2011**, *5*, 4145–4157.
38. P. Szabelski, W. Rżysko, T. Pańczyk, E. Ghijsens, K. Tahara, Y. Tobe, S. De Feyter, *RSC Advances*, **2013**, *3*, 25159-25165

39. M. Imoto, M. Takeda, A. Tamaki, H. Taniguchi, K. Mizuno, *Res. Chem. Intermed.* **2009,** *35*, 957-964.

40. G. Kresse, J. Furthmuller, *Phys. Rev. B*, **1996**, *54*, 11169-11186.

41. P. E. Blöchl, *Phys. Rev. B*, **1994**, *50*, 17953-17979.

42. J. P. Perdew, K. Burke, M. Ernzerhof, *Phys. Rev. Lett.*, **1996**, *77*, 3865-3868.

TOC

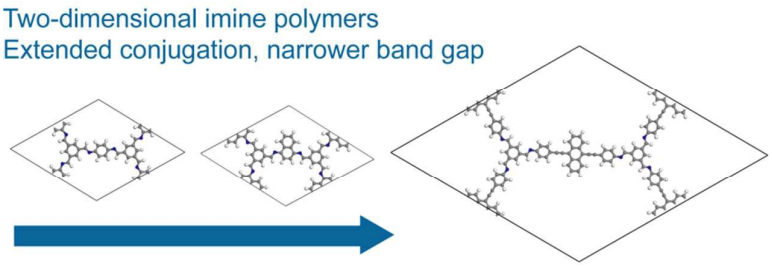


we introduce a strategy to tune the band gap of 2D imine polymers by adjusting the conjugation size of the monomer backbone, the structure of the designed 2D polymers were studied both theoretically and experimentally.